

Bruno Abart and Jean-François Sini
Laboratoire de Mécanique des Fluides UMR 6598,
Ecole Centrale de Nantes,
BP 92101, F-44321 Nantes Cedex 3, France.

ABSTRACT

The paper examines the computational modelling of the stably stratified atmosphere in the case of gravity wave breaking which induces turbulence generation and its transport in the whole atmosphere. The two first-order models developed for stably stratified flows by Abart and Sini, 1997 and validated on the LES of Kaltenbach et al., 1994 (stably stratified and shear flow) are applied to the simulation of the Boulder storm, 1972. In the atmosphere, the Reynolds number may be very high. An extension of the standard ϵ equation to these high Reynolds number allows to simulate the unsteady behaviour of the storm. The first-order models adapted to the stably stratified flows achieves well in the simulation of the generation, transport and diffusion of the turbulent kinetic energy k in the atmosphere contrary to the standard k - ϵ model and the k - L model where L is an integral length scale used to prescribe the dissipation rate ϵ .

1. INTRODUCTION

The effect of stable stratification (density decrease with height at faster rate than the adiabatic one) is of major importance in geophysical flows. The density decrease (increase of potential temperature with height) frequently diminishes turbulence which becomes more anisotropic and can strongly reduce the effective vertical diffusivity. Those stratification effects are due to some exchanges between turbulent kinetic energy (k) and potential energy:

$$E_{\text{pot}} = \frac{g}{\theta_0} \frac{\overline{\theta'^2}}{2\partial\theta/\partial z} \quad (1)$$

by means of the thermal vertical flux ($\overline{w'\theta'}$).

A k - ϵ - Ri_u and a 5-equation first-order closure models adapted for stratified flows were proposed in Abart and Sini, 1997. The k - ϵ - Ri_u model is a simple extension of the standard k - ϵ model introducing the turbulence Richardson number in order to take into account turbulence anisotropy caused by weak stratification (thermal turbulent diffusion is neglected). The 5-equation model, noted 5GL, is issued from second-order closures (Gibson and Launder, 1978, noted GL). The equations to solve are the ones for the turbulent kinetic energy (k), its dissipation rate (ϵ), the vertical turbulent kinetic energy ($\overline{w'^2}$), the vertical thermal flux ($\overline{w'\theta'}$) and temperature variance ($\overline{\theta'^2}$). The standard ϵ equation is not adapted to the atmospheric flows because it focusses on low to moderate Reynolds number (10 to 10^3). In the atmosphere, the Reynolds number can reach 10^8 . An original extension of the ϵ equation based on the modelling of

the tranfert time scale is proposed here: this extension is local and in agreement with the standard model.

The models are presented supposing the incompressibility. They are extended to the anelastic compressibility in order to apply them to the atmosphere.

On January 1972, the eastern slope of the Rocky Mountains experienced a severe Chinook windstorm due to gravity waves induced by stable stratification (Lilly, 1978). The simulation of this storm is achieved by our models and the standard models in order to simulate its unstationarity and turbulence. The comparison of the experimental dataset and the results of simulations to discuss the dissipation rate formulation and the hierarchy of the turbulence models in terms of the turbulence emergence and diffusion in the atmosphere.

2. k - ϵ - Ri_u MODEL

This first model, extension of the standard k - ϵ model, is based on a turbulence anisotropy parameterization for free shear part of turbulent normal stresses ($-2/3k$ in standard k - ϵ model) in terms of the horizontal turbulence Richardson number Ri_u (2).

2.1. Free Shear Part

An experimental correlation based on free shear grid turbulence decay affected by constant temperature gradient (Yoon and Warhaft, 1989's experiments) is built to provide a relation between the vertical turbulent Froude number Fr_t and the horizontal turbulent Richardson number Ri_u :

$$Fr_t = c Ri_u^{-n} \quad \text{with} \quad \begin{cases} Fr_t = \overline{w'^2}^{0.5} / NL_u \\ Ri_u = (NL_u)^2 / \overline{u'^2} \end{cases} \quad (2)$$

where N is the Brünt Väisälä frequency $-N^2 = (g/\theta_0)\partial\theta/\partial z$, $L_u = \overline{u'^2}^{1.5} / \epsilon$ the horizontal turbulence lengthscale and c and n are some simple functions of Ri_u .

In the experiments, Ri_u range from 0.0 to 70.0. Four zones can be approximately identified (fig. 1):

- turbulence isotropy for $Ri_u \leq 0.1$ («passive» flow).
- anisotropy increasing for $0.1 \leq Ri_u \leq 1.0$.
- return to isotropy for $1.0 \leq Ri_u \leq 30.0$.
- oscillations for Ri_u higher than 30.0; but, because of the too high complexity of oscillatory wave phenomenon at this closure level, these oscillations are not taken into account in the k - ϵ - Ri model and turbulence isotropy is imposed ($\overline{u'^2}_{FS} = 2/3k$).

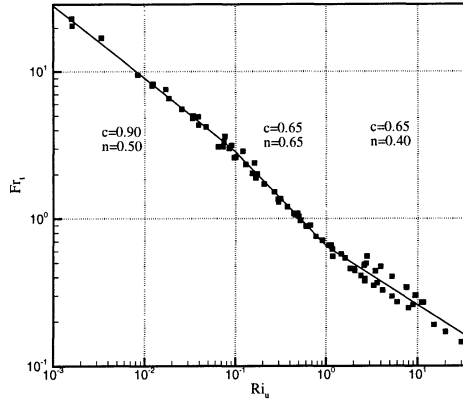


Fig. 1:

Ri_u function of Fr_t for experiments and correlation (2).

By using evident relation $\overline{w'^2}/\overline{u'^2} = Ri_u Fr_t^2$ based on number definition (2), the anisotropic parameterization is obtained:

$$\begin{cases} \overline{w'^2}_{FS}/\overline{u'^2}_{FS} = c^2 Ri_u^{-2n+1} \\ \overline{u'^2}_{FS} = \overline{v'^2}_{FS} \text{ (assu min g horizontal isotropy)} \\ 2k = \overline{u'^2} + \overline{v'^2} + \overline{w'^2} = 2\overline{u'^2}_{FS} + \overline{w'^2}_{FS} \end{cases} \quad (3)$$

In fact, system (3) is a simple anisotropic modelling for the first oscillatory wave (represented by the three first zones) of the kinetic/potential energy exchange phenomenon. So, thermal stratification has a direct influence on $\overline{u'^2}_i$.

2.2. Shear Part

Supposing cross derivatives preponderance, homogeneity hypothesis applied on $\overline{u'w'}$ second-order GL's transport equation gives:

$$\overline{u'w'} = -3/2 C_\mu \frac{k}{\epsilon} \left(\overline{u'^2} \frac{\partial W}{\partial x} + \overline{w'^2} \frac{\partial U}{\partial z} \right); \quad C_\mu = 0.09 \quad (4)$$

Generalization of (4) for shear part, $\overline{u'_i u'_j s}$, is adopted:

$$\overline{u'_i u'_j s} = \frac{3}{2} C_\mu \frac{k}{\epsilon} \left(P_{ij} - \frac{1}{3} P_{kk} \delta_{ij} \right) \quad (5)$$

In practice, supposing cross derivatives preponderance, the expression (5) reduces to (no sum on i and j (*)):

$$\overline{u'_i u'_j s} = -3/2 C_\mu \frac{k}{\epsilon} \left(\overline{u'^2} \frac{\partial U_j}{\partial x_i} + \overline{u'^2} \frac{\partial U_i}{\partial x_j} \right) + C_\mu \frac{k}{\epsilon} \overline{u'^2} \frac{\partial U_k}{\partial x_k} \delta_{ij} \quad (6)$$

As anisotropy of $\overline{u'^2}_i$ normal stresses due to stratification is taken into account by means of (3), we see that equation (6) sensibilize all the Reynolds stresses to stratification. Reminding that, in the standard k- ϵ model, $\overline{u'_i u'_j s} = -C_\mu k^2/\epsilon \cdot 2S_{ij}$ where S_{ij} is the strain rate tensor, the major improvement of this formulation is that it limits the over-estimation of turbulent kinetic energy production by shear in stably stratified flows.

* The indice notation is not strictly correct because of the simplifications or the privileged vertical direction. The indices i and j do not have to be summed.

Indeed, reduction of $\overline{w'^2}$ by stratification (equation (3)) imposes reduction of $\overline{u'w'}$ and so of shear production.

Using (6), supposing weak anisotropy, the anisotropic turbulent viscosity is (no sum on i and j (*)):

$$\nu_{Tij} = 3/2 C_\mu \frac{k}{\epsilon} \frac{\overline{u'^2}_i + \overline{u'^2}_j}{2} \quad (7)$$

2.3. Heat Fluxes

The modelling for vertical heat flux results from $\overline{w'^2}$ GL's transport equation using Rodi, 1985's type of hypotheses (applied on convection, diffusion and shear production terms). Then, $\overline{w'\theta'}$ depends on vertical turbulence anisotropy:

$$g/\theta_0 \overline{w'\theta'} = \frac{(C_1 - 1) \epsilon/k (\overline{w'^2} - 2/3 k)}{\overline{w'^2}/k - 2 + 4/3 C_3} \quad (8)$$

The equation (8) allows an estimation of the turbulent Prandtl number Pr_t to calculate the horizontal heat fluxes by means of usual gradient formulation with the anisotropic turbulent viscosity (7) (i=1 or 2(*)):

$$\begin{cases} Pr_t = -\frac{\nu_{T33}}{\overline{w'\theta'}} \frac{\partial \theta}{\partial z} \\ \overline{u'_i \theta'} = -\frac{\nu_{Tii}}{Pr_t} \frac{\partial \theta}{\partial x_i} \end{cases} \quad (9)$$

2.4. k and ϵ equations

The k equation is the standard one:

$$\frac{Dk}{Dt} = P_k + G_k - \epsilon + Dif_k \quad (10)$$

where P_k , G_k and Dif are respectively the shear production, the buoyancy production and the diffusion terms.

Let us recall that the standard model of the ϵ equation is issued from the first order Taylor expansion of the transfer time scale in function of the production time scale k/P_k and the turbulence time scale k/ϵ . For the stratified flows, the standard ϵ equation is:

$$\frac{D\epsilon}{Dt} = C_{\epsilon 1} \frac{\epsilon}{k} (P_k + C_{\epsilon 3} G_k) - C_{\epsilon 2} \frac{\epsilon^2}{k} + Dif_\epsilon \quad (11)$$

where $C_{\epsilon 3} = 0.2$ (Rodi, 1985).

At infinite Reynolds number, the limit ratio of the transfer time scale to the turbulence time scale is zero. The dissipation rate instantaneously adjusts itself to the k modifications. The k and ϵ equations are in equilibrium. Assuming that the transfer time scale is proportional to $k/(P_k + G_k - \epsilon)$ and to the turbulence Reynolds number $Re_T = k^2/(\nu\epsilon)$ at high Reynolds number, the sum of the model for moderate Reynolds number and the model for high Reynolds number provides the ϵ transport equation:

$$\begin{aligned} \frac{D\epsilon}{Dt} = C_{\epsilon 1} \frac{\epsilon}{k} (P_k + C_{\epsilon 3} G_k) - C_{\epsilon 2} \frac{\epsilon^2}{k} + Dif_\epsilon \\ + C_{\epsilon 4} \frac{\epsilon}{k} (P_k + G_k - \epsilon) Re_T^{1/2} \end{aligned} \quad (12)$$

The coefficients are supposed to be constant (Table 1) and are determined like in the standard model with the grid generated turbulence decrease requirements- the slope n is -2.0 for $Re_T = 1$ and -1.1 for $Re_T = 100$ (Comte-Bellot and Corrsin, 1966)- and the neutral constant flux layer requirements. So, this model for high Reynolds number and the standard model for moderate Reynolds number are linked up. Let us note that the

high Reynolds ϵ equation model is the standard one with some coefficients which are functions of Re_T .

models:	C_μ	σ_k	σ_ϵ	$C_{\epsilon 1}$	$C_{\epsilon 2}$	$C_{\epsilon 3}$
standard	0.09	1.0	1.3	1.44	1.92	0.00
high Reynolds number	0.09	1.0	1.3	1.04	1.45	0.05

Table 1: Coefficients of the standard and high Reynolds number ϵ equation models.

3. THE FIVE EQUATION MODEL

Anisotropisation by stratification is due to kinetic/potential energy exchanges by means of vertical heat flux. That is why we built a five equation model based on the explicit resolution of the three further transport equation for $\overline{w'^2}$, $\overline{w'\theta'}$ and $\overline{\theta'^2}$. The basis second-order model for thermal flows (GL) provides these transport equation.

The other unknown Reynolds stresses are estimated by (no sum on i and j (*)):

$$\overline{u'_i u'_j} = \left(k - 1/2 \overline{w'^2} \right) \delta_{ij} - 3/2 C_\mu \frac{k}{\epsilon} \left(\overline{u'_i} \frac{\partial U_j}{\partial x_i} + \overline{u'_j} \frac{\partial U_i}{\partial x_j} \right) + 3/2 C_\mu \frac{k}{\epsilon} \left(\overline{u'^2} \frac{\partial U}{\partial x} + \overline{v'^2} \frac{\partial V}{\partial y} \right) \delta_{ij} \quad (13)$$

Equation (13), with the same shear part that of the $k-\epsilon-Ri_u$ model (6), allows the vanishing into two component turbulence (extinction of $\overline{w'^2}$, $\overline{w'\theta'}$ and $\overline{u'w'}$).

The k and ϵ transport equations are the same as used in the $k-\epsilon-Ri_u$ model, i.e. equations (10) and (12).

4. ANELASTIC COMPRESSIBILITY

The Boussinesq approximation is applied on the Navier-Stokes equations. The reference density, noted ρ_r , is the density of a hydrostatic and adiabatic atmosphere. The continuity equation is reduced to its anelastic form, $\partial(\rho_r u_i)/\partial x_i = 0$. The diagnostic and prognostic equations of the turbulence correlations presented in the previous paragraphs are built supposing the incompressibility, i.e. $\partial u_i / \partial x_i = 0$. These equations are written in the anelastic approximation introducing ρ_r in the time and space derivatives. The reference density acts as a stretching function on the turbulence structure.

5. THE BOULDER STORM

5.1 Description and experimental analysis

On January 1972, the eastern slope of the Rocky Mountains of northern Colorado and Southern Wyoming experienced a severe Chinook windstorm. Wind speeds of around 50 m/s are recorded in populated areas of Boulder. Beside stationary vertical temperature and wind soundings at Gran Junction, 300km west (upstream) of Boulder, the windstorm was unstationary with the formation of two high wind speed core on the mountain lee side. The two surges were of roughly the same intensity and time spaced out of two hours. This storm was generated by the breaking gravity waves appearing because of the positive temperature vertical profile.

The experimental dataset is issued from two instrumented aircraft flights: the first at 9000m during the first part of the storm and the second at 6000m during the second part of the storm (Lilly, 1978). This dataset was analyzed with the assumption that the flow is two-dimensional and steady. Figure 2 shows the time averaged horizontal velocity and Table 2 shows the estimation of the perturbation kinetic energy with respect to the time averaged velocity components at 6000m.

5.2 Geometry and computation conditions

The atmospheric code SUBMESO is used to simulate the Boulder storm. This model allows to simulate the dynamical, chemical and micro-physical processes of the meso and sub-meso scales of the atmosphere. This atmospheric code is issued from the ARPS code of CAPS (Xue et al., 1995).

The geometry - a simplified bell shape mountain of 2000m height and of 10000m half width-, the initial and upstream boundary wind speed and temperature - the Gran Junction soundings- in previous simulations are selected in our simulation (Klemp and Lilly, 1978; Durran and Klemp, 1983; Bougeault and Lacarrère, 1989; Thunis, 1998). The simulation domain horizontal and vertical lengths are respectively 120km and 18km; the discretization of the domain is made by 73×43 points like in the previous simulations. The time step is 0.5s instead of 30s in the previous simulations because we do not use artificial viscosities.

Indeed, in this strongly advective simulation, the numerical method used to stabilize the advective terms is highly determining. In all the simulations cited above, some high artificial viscosities are imposed to avoid the numerical oscillations. This method leads to the reduction of the gravity wave and the slowing down of the time evolution of the windstorm. To add, the inflow and outflow absorbing layers on the potential temperature and the velocity components are avoided. Indeed, as they drastically diffused the outgoing wind vortices, the first high wind speed core does not go out of the domain and the windstorm becomes stationary. On this flow, the code SUBMESO is numerically stable beside the intense time and space perturbations of the fields of potential temperature and velocity.

5.3 Comparison with the experimental dataset

At the opposite of the previous simulations, our numerical solutions are unstationary because there are no artificial viscosities. The Figure 2 illustrates this behavior for the high Reynolds number $k-\epsilon$ model. In order to compare the numerical results with the experimental dataset, a time average operator is used, the definition of which is:

$$\langle \Phi(t) \rangle = \int_{t_1}^{t_2} \Phi(t) dt \quad (14)$$

where Φ is a Reynolds averaged field. The time t_1 is the beginning of the windstorm; it is chosen at the beginning of the descent of stratospheric air ($t_1 = 1h30$ of numerical integration time). The time t_2 is chosen after that two surges has passed over Boulder ($t_2 = 6h$ of numerical integration time) for the simulation with the turbulence model 5GL.

The Figure 3 shows the time averaged solution of the horizontal velocity $\langle U(t) \rangle$ issued from the analysis of Lilly, 1972. This solution is analytically obtained with the measurements and the mass conservation equation. The primary stratospheric wave was measured by the aircrafts and the high wind speed core was deduced by mass conservation. The Figure 4 shows the time averaged horizontal velocity provided by the $k-\epsilon$ and $k-\epsilon-Ri_u$ turbulence models with the high Reynolds number ϵ equation and the $k-L$ model (Bougeault and Lacarrère, 1989) where L is a vertical integral length scale. This length scale is a function of the perturbation of potential temperature with respect to the reference potential temperature.

The result provided by the 5GL model is very closed to the $k-\epsilon-Ri_u$ model (not shown). The primary stratospheric wave is well simulated by all the models except by the $k-L$ model because of the dissipation rate algebraical modelling (see 5.4). The measured average minimum value of $\langle U(t) \rangle$ is closed to -

3m/s. This minimum is overestimated by the k- ϵ model (-12.2m/s) because this model overestimates the variations of turbulent kinetic energy in the breaking zone. Indeed, the vertical heat flux is overestimated by the standard model of $\overline{w'\theta'}$; so, k is overpredicted in the instable zones and underpredicted in the stable zones. The k- ϵ - Ri_θ model provides -3.75m/s because k is transported in the stable zones (see 5.5) and consequently, its variations are lower than with the k- ϵ model.

The Table 2 shows the time averaged kinetic energy of the velocity perturbations, i.e. the velocity variance $1/2 < U_i(t) - \langle U_i(t) \rangle >^2$ at the vertical of Boulder ($x=50\text{km}$ and $z=6\text{km}$) for the experiment and the numerical simulations. The experimental value is issued from the space energy spectrum computed with the data of a 30min horizontal flight at 6km during the second part of the storm (movements of the high wind speed cores in the surface layer). This perturbation kinetic energy PTK is obtained by the integration of the space energy spectrum for the length scales higher than 1km. This variance is the atmospheric kinetic energy turbulence. The variance is very underestimated with the k-L model because after the descent of the stratospheric air, the flow restratifies (behavior in agreement with Thunis, 1999). The PTK is overestimated by the k- ϵ model because of the overestimation of the turbulent kinetic energy variations. The k- ϵ - Ri_θ model and the 5GL model shows a quite good agreement with the measurements.

5.4 Discussion on the high Reynolds number formulation

The Figure 5 shows the horizontal velocity $U(t)$ when the two high wind speed cores moves on the ground ($t=5\text{h}$) for the standard k- ϵ model, the high Reynolds number k- ϵ model and the k-L model. For the high Reynolds k- ϵ model, the two cores are simulated. For the standard k- ϵ model, the overestimation of ϵ with respect to k limits the transport of k and consequently, limits the movements of the primary stratospheric wave which initializes the displacement of the first high wind speed core in the surface layer. The k-L model follows the same type of behaviour except in the breaking zone where the turbulent kinetic energy is very high (Figure 6d). In fact, the turbulence length scale provided by the k-L model is much higher than the turbulence length scale k/ϵ of the k- ϵ type models. The mixing of the flow by the turbulence limits the development of the first high wind speed core. We point out that the use of an integral length scale forces the turbulence length scale to be closed to the average velocity and potential temperature time scales. So, the flow is less unsteady and an important part of the velocity perturbations are integrated in the turbulent kinetic energy. This is evidently not the case when a local ϵ transport equation is selected.

5.5 Discussion on the turbulence models

The Figure 6 shows the turbulent kinetic energy when the primary stratospheric wave is fully developed ($t=3\text{h}$) for all the models. At this time, the stratospheric turbulence is issued from the wave breaking at the vertical of Boulder ($x=50\text{km}$). The turbulence reports received during the storm from various civilian and military aircraft over central Colorado revealed that the turbulent kinetic energy was diffused and transported up to Denver ($x=70\text{km}$) in the surface layer and in the stratosphere. For the high Reynolds number k- ϵ model, the turbulent zone is limited to the breaking zone; k is less transported in the stratified zones than with the high Reynolds number k- ϵ - Ri_θ model because of the modelling of the vertical heat flux which

participates to the destruction of k in the stable zones. Indeed, for the high Reynolds number k- ϵ - Ri_θ model, the vertical heat flux is zero at high stratification because the turbulence becomes isotropic (equation (8)). The decrease of $\overline{w'\theta'}$ allows the transport of k in the stable zones after the primary stratospheric wave ($x > 60\text{km}$). The k production and transport is qualitatively predicted by the 5GL model and in agreement with the observed turbulence (Figure 3): k is produced in the second part of the stratospheric wave (positive vertical velocity part at $x \approx 50\text{km}$), in the high wind speed core ($x \approx 50\text{km}$, $z \approx 2000\text{m}$) and in the instable zone in the surface layer ($x \approx 70\text{km}$, $z \approx 2000\text{m}$). Then, k is transported to the stable zones.

5. CONCLUSIONS

The following conclusions can be drawn from this qualification for the stable stratified atmosphere of the first-order closures presented here:

- the k- ϵ - Ri model, extension of standard k- ϵ one, is better in transporting k in the stable layers than this latter.
- beside its complexity, the five equation models is numerically stable if the realizability conditions are explicitly imposed after each time step; this model achieves well in representing the turbulent kinetic energy. This model can be used for preliminary studies on the aircraft routes in such gravity wave storms (let us note the layer with the minimum of turbulence at $z \approx 4000 - 5000\text{m}$ on the Figure 6c).
- the numerical diffusion has to be avoided in the numerical code in order to simulate the unstationarity of the atmospheric flows.
- the high Reynolds number ϵ equation modelling allows to take into account the simultaneous k and ϵ equilibrium at infinite Reynolds number and allows to simulate the development of the Boulder storm in the surface layer.

REFERENCES

- Abart, B., and J.F. Sini, 1997, «New first-order closure for stably stratified flows.» *Eleventh Symposium on Turbulent Shear Flows*, Grenoble, France, **2**, p. P2.1-P2.6.
- Bougeault, P., and P. Lacarrère, 1989 «Parameterization of orography-induced turbulence in a mesobeta-scale model», *Mon. Wea. Rev.* **117**, p. 1872-1890.
- Comte-Bellot, G., and S. Corrsin, 1966, «The use of a contraction to improve the isotropy of grid generated turbulence, *J. Fluid Mech.*, **25**, p. 657.
- Durran, D.R., and J.B. Klemp, 1983, "A compressible model for the simulation of moist mountain wave", *Mon. Wea. Rev.* **111**, p. 2341-2361
- Gibson, M.M., and Launder, B.E., 1978, "Ground effects on pressure fluctuations in the atmospheric boundary layer." *J. Fluid Mechanics*, **86**, p. 491-511.
- Kaltenbach, H.-J., T. Gerz and U. Shumann, 1994, «Large-eddy simulation of homogeneous turbulence and diffusion in stably stratified shear flow.» *J. Fluid Mech.*, **280**, p. 1-40.
- Lilly, D.K., 1978, "A severe downslope windstorm and aircraft turbulence event induced by a mountain wave", *J. Atmos. Sci.* **35**, p. 59-77.
- Rodi, W., 1985, "Calculation of stably stratified shear layer flows with a buoyancy-extended k- ϵ turbulence model." *Turbulence and Diffusion in Stable Environment*, ed. J.H. Hunt, Oxford University Press, New York, p. 111-143.
- Thunis, P., 1998, «Formulation of a nonhydrostatic vorticity model (TVM), and application to topographic waves and to the 1972 Boulder wind storm, » *J. Atmos. Sci.*

Xue, M., K.K. Droegemeier, V. Wong, A. Shapiro, K. Brewster, 1995: «Advanced Regional Prediction System ARPS User's Guide. Version 4.0.» Center for Analysis and Prediction of Storms, The University of Oklahoma, 380 pp.

Yoon, K., and Warhaft, Z., 1990, "The evolution of grid-generated turbulence under conditions of stable thermal stratification." *J. Fluid Mechanics*, **215**, p. 601-638.

	PTE (m^2s^{-2})
dataset analysis	≈ 150.0
standard model	93.9
k-L model	48.1
high Re_T k- ϵ model	183.9
high Re_T k- ϵ - Ri_u model	168.13
high Re_T 5GL model	142.0

Table 2: Perturbation kinetic energy at $x = 50\text{km}$, $z = 6000\text{m}$, $\text{PKE} = 1/2 < U_i(t) - < U_i(t) >>^2$ (see Paragraphe 5.3).

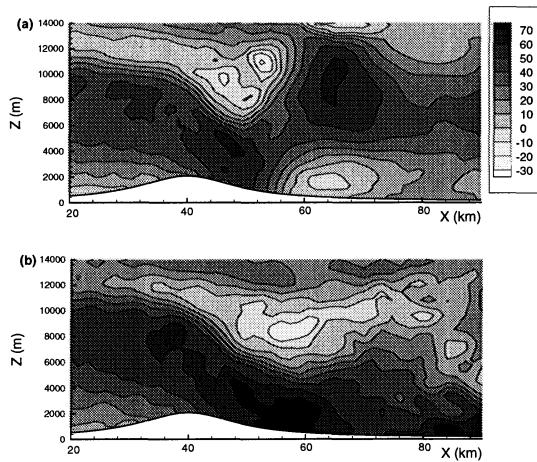


Figure 2: Detail of the horizontal velocity $U(t)$ near the mountain after (a) $t=3\text{h}30$ and (b) $t=6\text{h}$ of integration time for the high Reynolds number k- ϵ model. (a) shows the development of the primary stratospheric wave and (b) shows the movement of the two high wind speed cores on the ground.

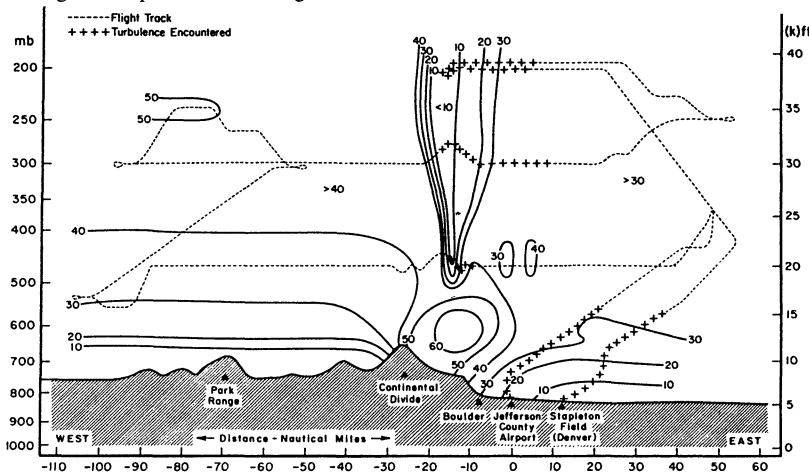


Figure 3: Analysis of westerly wind component (ms^{-1}) on 11 January 1972, made from the one aircraft and sonde data. The analysis below 470mb (the surface layer) was deduced from the mass conservation equation with the assumptions that the flow is two-dimensional and steady (from Lilly, 1978).

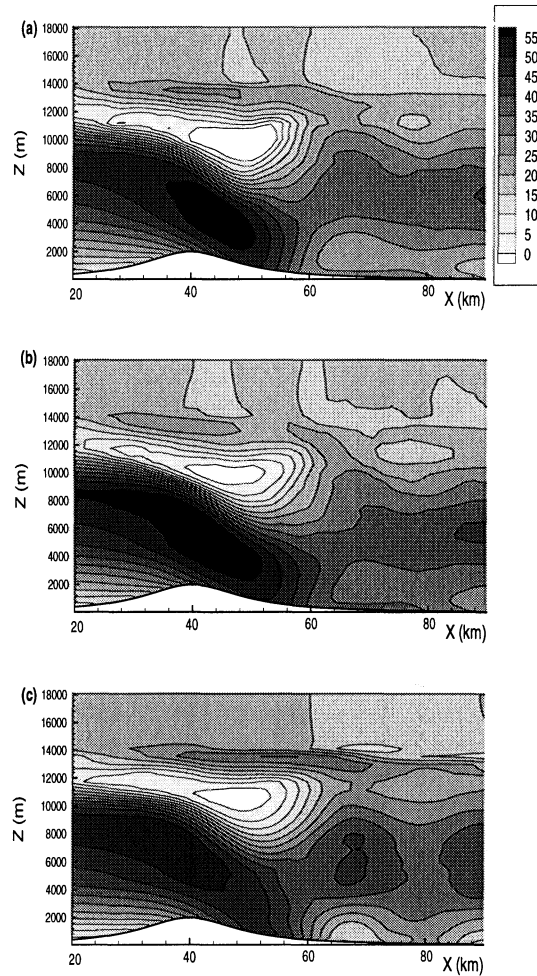


Figure 4: Time averaged horizontal velocity $<U(t)>$ provided by (a) the k- ϵ and (b) k- ϵ - Ri_u turbulence models with the high Reynolds number ϵ equation and (c) the k-L model.

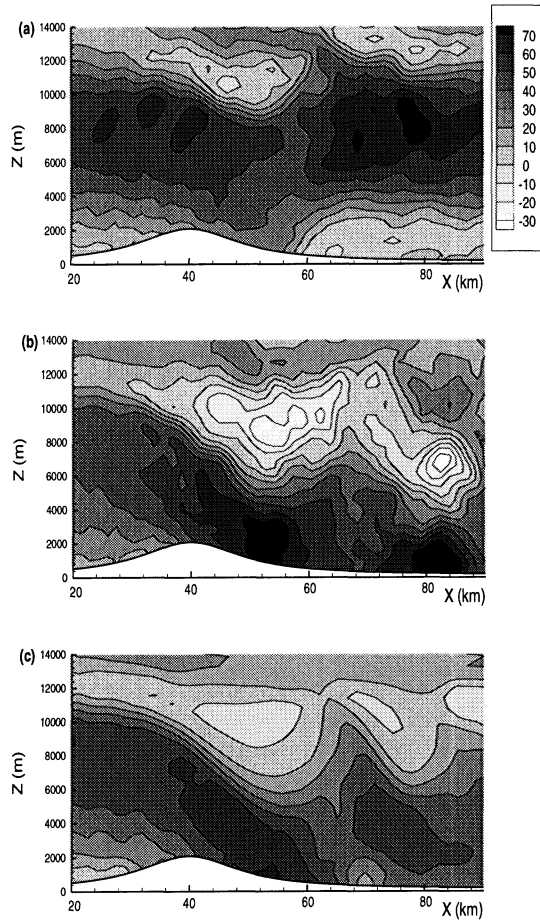


Figure 5: Detail of the horizontal velocity $U(t)$ near the mountain after $t=5h$ of integration time for (a) the standard $k-\epsilon$ model, (b) the high Reynolds number $k-\epsilon$ model and (c) the $k-L$ model.

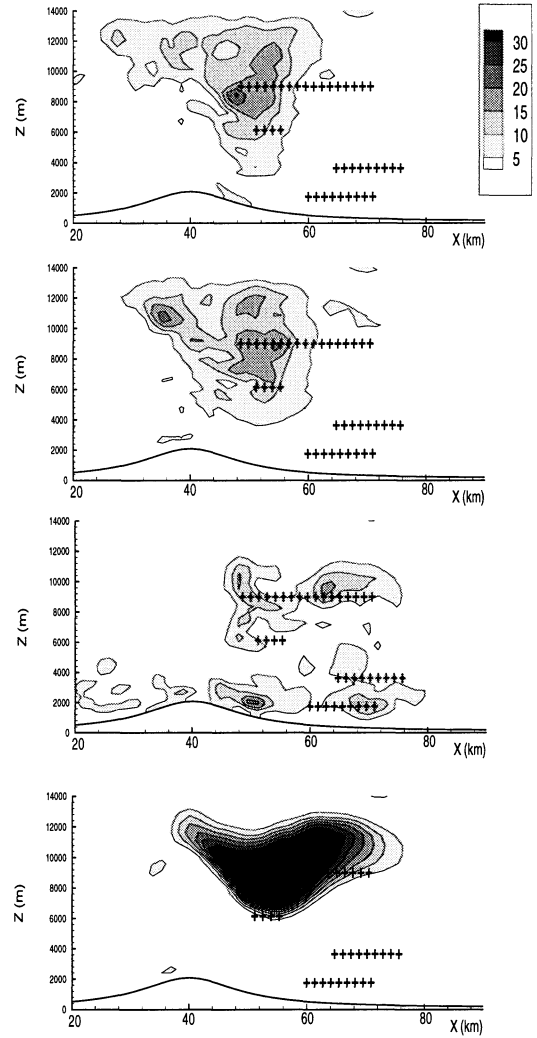


Figure 6: Detail of the turbulent kinetic energy (m^2s^{-2}) after $t=3h$ of integration time for (a) the high Reynolds number $k-\epsilon$ model, (b) the high Reynolds number $k-\epsilon-Ri_u$ model, (c) the high Reynolds number 5GL model and (d) the $k-L$ model. The pluses show the periods of significant turbulence during the aircraft track (from Lilly, 1978).